

Superconducting and magnetic behaviour of niobium doped $\text{RuSr}_2\text{Gd}_{1.5}\text{Ce}_{0.5}\text{Cu}_2\text{O}_{10-\delta}$

C A Cardoso^{1,4}, F M Araujo-Moreira¹, V P S Awana², H Kishan² and O F de Lima³

¹ Departamento de Física, UFSCar, São Carlos—SP, 13565-905, Brazil

² National Physical Laboratory, Dr K S Krishnan Marg, New Delhi 110012, India

³ Instituto de Física 'Gleb Wataghin', UNICAMP, Campinas—SP, 13083-970, Brazil

Received 30 January 2007, in final form 19 March 2007

Published 13 April 2007

Online at stacks.iop.org/JPhysCM/19/186225

Abstract

Polycrystalline samples of $\text{Ru}_{1-x}\text{Nb}_x\text{Sr}_2\text{Gd}_{1.5}\text{Ce}_{0.5}\text{Cu}_2\text{O}_{10-\delta}$, $0 \leq x \leq 0.5$, have been synthesized and structurally characterized by x-ray diffraction (XRD). Resistivity, magnetization and AC susceptibility measurements have been done and analysed considering a phase separation scenario. A strong suppression of the cluster glass (CG) transition associated with niobium doping was identified. In fact, the CG phase was not present in samples for $x \geq 0.2$, leading to changes in the magnetic hysteresis loops measured at low temperatures. These hysteresis loops can be explained as a result of the contribution of two distinct magnetic phases: the canted AFM phase and embedded Ru^{4+} -rich clusters which order as a CG in low temperatures. Interestingly, the significant changes in the magnetic response of the material do affect the superconducting transition temperature T_c . It was found that both T_c and the superconducting fraction are reduced in samples which present the spin glass phase. Therefore, our results point to some coupling between magnetism and superconductivity in this ruthenocuprate family, the presence of the magnetic moment being deleterious for the superconductivity.

(Some figures in this article are in colour only in the electronic version)

1. Introduction

The ruthenocuprate family of composition $\text{RuSr}_2\text{Gd}_{1.5}\text{Ce}_{0.5}\text{Cu}_2\text{O}_{10-\delta}$ (Ru-1222) has attracted considerable interest because of its fascinating and complex magnetic and superconducting properties. Besides the possible coexistence of superconductivity and magnetic order in ruthenocuprates [1, 2], a proper understanding of their magnetic behaviour has challenged researchers in recent years and no definitive agreement about these questions has been

⁴ Author to whom any correspondence should be addressed.

reached yet [3, 4]. The magnetic behaviour of Ru-1222 presents three major features: an antiferromagnetic transition at temperatures around 160–180 K, a spin glass-like transition around 70–90 K and a superconducting transition at temperatures close to 40 K [4–6]. However, a detailed and more fundamental interpretation of these features is still lacking. In particular, some recent results point towards a scenario of multiple magnetic phases, where different regions of the sample may present different magnetic behaviour [7–10]. The discussion becomes even more complicated if one takes into consideration the possible influence of secondary phases, sample inhomogeneity and oxygen non-stoichiometry on the overall magnetic response of the studied samples [3, 6, 11].

Studies in this area have mainly employed two basic approaches. The first one probes the properties of a standard sample using different techniques, which should provide complementary information sufficient to reinforce or discard a specific model. Important results have been obtained in this way, although sometimes the attempts to correlate results from different groups have led to contradictions [7–9, 12–17]. A second approach is the study of chemically altered compounds, where by proper chemical substitutions one can control relevant parameters that affect the sample's properties and, in this way, get a better understanding of the mechanisms involved in it [18–27]. This second approach is particularly interesting for exploring the possible microscopic coexistence of superconductivity and magnetic order in the ruthenocuprate family.

The fact that superconductivity occurs in the CuO_2 planes while magnetic order is restricted to Ru ions in the RuO_2 planes casts some doubt on the genuine coexistence of these two phenomena at a microscopic level. A simple way to explore this issue is to chemically modify one of these families of planes keeping the other one unaffected. Zinc substitution for Cu in Ru-1222 polycrystals, for instance, causes a strong suppression of its superconductivity response but does not significantly affect the magnetic order, indicating that these two phenomena are practically decoupled [18].

Substitutions in the Ru site can be used to investigate both magnetic order and superconductivity. Examples are the heterovalent substitutions by Sb [19], Pb [20], Sn [21] Mo [22] or Co [23] that affect the carrier density in the CuO_2 planes and the magnetic coupling between the Ru ions. As a consequence, in these substitutions it is difficult to separate the possible genuine coexistence of superconductivity and magnetic order. More interesting is Nb substitution for Ru [26, 27], since in this case both ions have valence close to 5+ and changes in the carrier density should be much smaller than in the previous examples. It has been found that the superconducting transition is not affected by Nb substitution even when the magnetic moment is drastically reduced [26, 27]. This result could be interpreted as evidence that magnetism and superconductivity are decoupled in Ru-1222. However, more detailed studies on the magnetic behaviour of Nb-doped Ru-1222 (Ru-1222:Nb) are certainly desirable, to help us understand the complex interplay between superconductivity and magnetism in this system. As will be shown in the present work, it is possible to conclude that superconductivity and magnetism are indeed coupled in Ru-1222:Nb if one looks carefully at the obtained data.

It is also interesting to compare the results for doped Ru-1222 with studies in Ru-1212. Even considering the differences between both compounds, it is curious that similar studies for Ru-1212:Nb samples present a significant change in the superconducting transition temperature with Nb and Sn doping [28–30]. Such change, however, was explained by considering the effect of these substitutions on the hole concentration in the CuO_2 layers [30]. Therefore, reduction of the magnetic moment in the RuO_2 layers does not seem to play any role at all in the case of Ru-1212:Nb. In the present work we explore the magnetic behaviour of $\text{Ru}_{1-x}\text{Nb}_x\text{Sr}_2\text{Gd}_{1.5}\text{Ce}_{0.5}\text{Cu}_2\text{O}_{10-\delta}$ samples with Nb substitution up to $x = 0.5$, which was found to be its solubility limit. The blocking temperature of the cluster glass (CG) phase is

strongly reduced with increase in the Nb content, and no indication of the CG transition at all is present for substitutions higher than $x = 0.2$. The AFM transition is also affected by the Nb substitution, but in a gentler way than the CG transition. As a result, the overall magnetic signal of the samples is greatly reduced and a diamagnetic response due to the superconducting component is clearly detected at temperatures below T_c for $x > 0.1$ samples. However, a close inspection of the superconducting response has shown a small reduction in T_c for the samples with higher magnetic signal (the ones which present the CG phase). This change could not be associated just with the influence of Nb substitution on the charge doping in the CuO_2 planes, and is possibly an indication of the correlation between magnetism and superconductivity in Ru-1222.

2. Experimental details

Samples of composition $\text{Ru}_{1-x}\text{Nb}_x\text{Sr}_2\text{Gd}_{1.5}\text{Ce}_{0.5}\text{Cu}_2\text{O}_{10-\delta}$ were synthesized through a solid-state reaction route from stoichiometric amounts of RuO_2 , SrO_2 , Gd_2O_3 , CeO_2 , CuO and Nb_2O_5 . Calcinations were carried out on the mixed powders at 1000, 1020 and 1040 °C for 24 h at each temperature with intermediate grindings. Following this, the pressed bar-shaped pellets were annealed in flowing oxygen at 1075 °C for 40 h and subsequently cooled slowly over a span of 20 h down to room temperature. The same pellets were further annealed in flow of O_2 , at atmospheric pressure and 400 °C, for 24 h, and slowly cooled to room temperature, in the same environment over a span of 6 h. The final samples were characterized and found to be almost single phase materials up to $x = 0.50$, whose properties will be discussed in section 3. X-ray diffraction (XRD) patterns were obtained using $\text{Cu K}\alpha$ radiation at room temperature for all samples. AC susceptibility measurements were performed in a commercial PPMS (physical properties measurement system), while for the DC measurements a SQUID magnetometer (MPMS-5) was employed, both items of equipment being made by Quantum Design. The four-point technique was used for the resistivity measurements, in a conventional He^4 cryostat.

3. Results and discussion

Figure 1 presents the XRD results for all samples. The observed peaks were correlated with the expected ruthenocuprate phase. Within the XRD resolution, no secondary phases containing Nb could be detected even for $x = 0.5$, indicating that niobium was successfully incorporated in the Ru-1222:Nb phase up to this concentration. For higher Nb contents ($x > 0.5$) we could not get the required pure phase using the heat treating schedules applied in the present study. Small amounts of $\text{RuSr}_2\text{GdCu}_2\text{O}_8$ and $\text{RuSr}_2\text{GdO}_6$ are indexed to a few small peaks, as indicated in figure 1. The presence of small amounts of secondary phases is commonly observed even in undoped samples, as previously reported. In fact, our currently studied samples present a phase purity comparable to those reported earlier by various authors [1, 7–9, 14, 20, 21, 27]. As far as the lattice parameters are concerned, an increase in them is seen since the ionic size of Nb^{5+} is larger than that of the Ru^{5+} ion. The undoped compound ($x = 0$) has its lattice parameters $a = b = 3.835(2)$ Å and $c = 28.573(6)$ Å. On the other hand, for the Nb-substituted ($x = 0.5$) compound $a = b = 3.851(5)$ Å and $c = 28.715(4)$ Å, in agreement with [27].

The superconducting transition temperature (T_c) was determined through resistivity and AC magnetic susceptibility (figures 2 and 3, respectively). For the resistive transitions (figure 2) T_c was defined at the point where the resistance extrapolates to zero. For the AC susceptibility measurements T_c was defined at a clear step that appears in the real component, as will be discussed later in more detail. As shown in the inset of figure 2, the increase in niobium

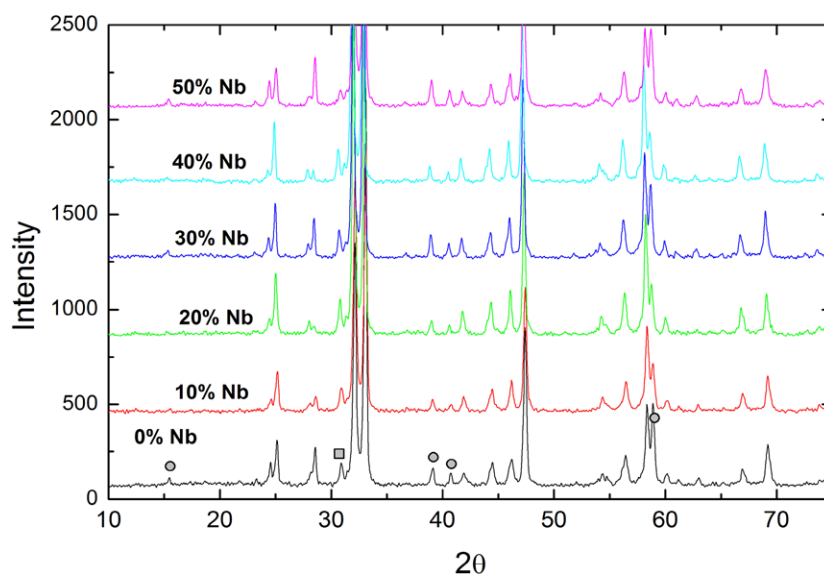


Figure 1. X-ray diffraction patterns for samples with different niobium content. Peaks associated only with secondary phases are indicated with circles ($\text{RuSr}_2\text{GdCu}_2\text{O}_8$) or squares ($\text{RuSr}_2\text{GdO}_6$) in the undoped sample. Each spectrum was shifted vertically by approximately 1/5 of the height of the most intense peak for the sake of clarity and to allow the identification of the impurity peaks.

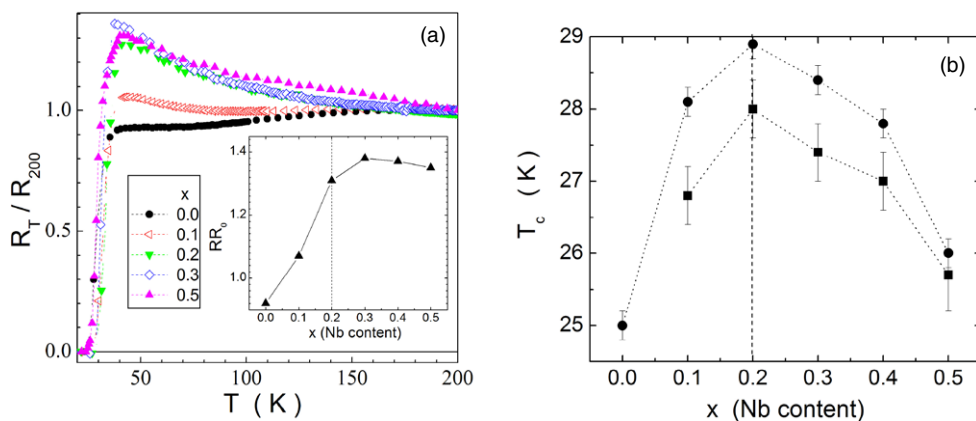


Figure 2. (a) Normalized resistance as a function of temperature. The inset shows the dependence of the resistivity ratio (RR_0) with Nb content. (b) Superconducting transition temperature T_c as a function of Nb content, estimated from resistivity (circles) and AC magnetic susceptibility (squares).

content from $x = 0.0$ to 0.5 leads to an increase in the resistivity ratio at the onset of transition (RR_0), and the samples change from a metallic to semiconducting behaviour. That is expected if niobium with valence 5^+ replaces ruthenium with valence smaller than 5^+ . In that way, the density of charge carriers is reduced with niobium doping, leading to the semiconducting behaviour. In fact, it is well known that ruthenium ions present an average valence smaller than 5^+ , as indicated in previous studies [31–33]. However, the reported values for ruthenium valence change from sample to sample, possibly due to changes in the oxygen content of each specific sample. More interesting is the behaviour of the superconducting transition

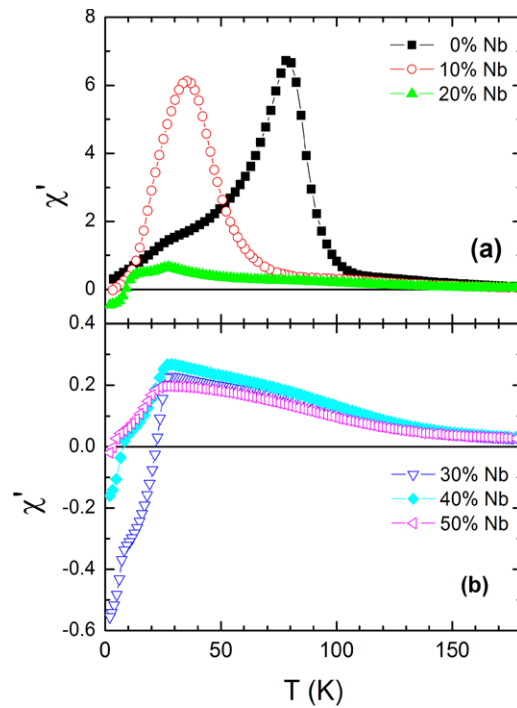


Figure 3. Real part of the AC susceptibility for lightly (a) and heavily (b) Nb-doped samples. The large peaks in the curves for pure and 10% Nb substitution samples are related with the occurrence of the cluster glass transition, and are not observed for samples with higher Nb content. The increase in χ' at approximately 160 K is associated with the AFM transition.

temperature with doping, shown in figure 2(b). Although at first sight T_c seems to remain constant, a close inspection of the plot in figure 2 reveals that T_c actually increases from 25 K, at $x = 0.0$, up to 29 K, at $x = 0.2$, and then reduces back to 26 K, at $x = 0.5$ (see figure 2(b)). The reduction of charge carriers with the increase in niobium doping would suggest a monotonic reduction in T_c as x increases, so the hole doping effect alone cannot explain the increase in T_c for low Nb content and its maximum for $x = 0.2$, unless this specific hole concentration corresponds to the optimum doping level for this superconductor. It is important to notice that this trend was confirmed by AC susceptibility measurements as shown in figures 2(b) and 3. Also, changing the criteria used to define T_c does not qualitatively affect the results. For instance, defining T_c at the inflection point of the resistivity transition gives $T_c = 28$ K for $x = 0.0$, increasing up to a maximum of $T_c = 34.4$ K for $x = 0.2$, and then reducing to $T_c = 29$ K for $x = 0.5$. Finally, estimations of the error associated with the procedure to determine T_c (see error bars in figure 2(b)) indicate that the observed changes in T_c are meaningful, although small.

Figure 3 presents the temperature dependence of the real part of the complex AC susceptibility $\chi_{ac} = \chi' + i\chi''$. For the sake of clarity, the measurements were divided in two groups, one for the lightly doped samples ($0 \leq x \leq 0.2$, figure 3(a)) and a second one for the heavily doped samples ($0.3 \leq x \leq 0.5$, figure 3(b)). The value $x = 0.2$ was chosen to divide the samples in two groups since this corresponds to the maximum observed in T_c , as shown in figure 2(b). All χ_{ac} measurements were performed at an applied field of $H = 50$ Oe, while the amplitude and frequency of the excitation field were kept constant at 1 Oe and 1 kHz,

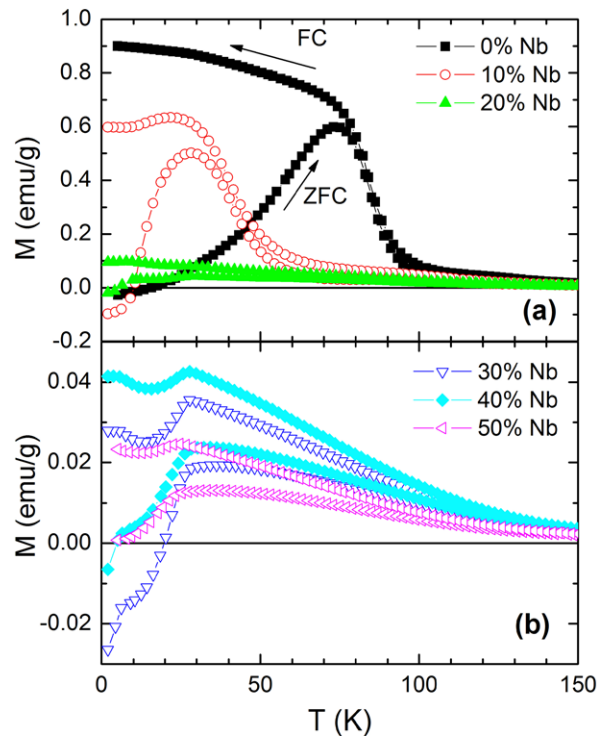


Figure 4. DC magnetization as a function of temperature for lightly (a) and heavily (b) doped samples, for $H = 50$ Oe. The total magnetic moment is much larger for samples with a niobium content below 10%, which causes the pair-breaking effect responsible for a partial suppression of the superconducting response for those samples.

respectively. All $\chi'(T)$ curves present a change in their slope at temperatures around 160 K, which is associated with the antiferromagnetic transition of a fraction of the sample. Large peaks in χ' can be seen at approximately 80 and 35 K for the $x = 0$ and 0.1 samples, respectively. The positions of these peaks indicate the blocking temperature of the cluster glass phase. Samples with higher niobium contents do not present the cluster glass transition at all. Therefore, it is clear that niobium substitution leads to a strong suppression of the cluster glass transition. The superconducting transition takes place in two steps. The first step occurs at temperatures between 25 and 29 K and corresponds to the onset of superconductivity inside the grains of our polycrystalline sample. The obtained T_c values, already presented and discussed in figure 2, were determined from this first transition. The strong magnetic signal for the $x = 0.0$ sample is a serious obstacle for a reliable determination of T_c in this case. The second step in the superconducting transition, observed at a lower temperature, corresponds to an intergrain transition. These two steps can be easily identified in the AC susceptibility measurements (figure 3) and they are also present in the magnetization curves (figure 4), although in this latter case the superposition of the magnetic signal from the Ru sublattice creates difficulties for the analysis of the superconducting response. The intergrain transition occurs at different temperatures for each sample, which is usual for polycrystalline samples [34]. Observe that none of the transitions have taken place at temperatures close to 9 K, which excludes the possibility of Nb segregation, in agreement with the absence of any peak associated with Nb in the XRD analysis.

We also explored the frequency dependence of the AC susceptibility in the range of 100 Hz to 10 kHz (not shown). We observed that the shifts with frequency of the peaks observed in the measurements for $x = 0$ and 0.1 samples were consistent with the expected behaviour of a cluster glass, in agreement with our previous reports [4–6]. The other samples studied in this work do not present such a cluster glass peak in χ' and a small change with frequency was only observed in the vicinity of the intergranular superconducting transition, as expected for polycrystalline superconductors [34]. Another interesting result is that the intensity of the drop in the χ' curves, related to the superconducting transition, is significantly reduced with increase in the doping level. This indicates a reduction in the overall superconducting volume as the Nb content is increased.

The temperature dependence of the magnetization for all samples is shown in figure 4. The samples were cooled in zero magnetic field down to the lowest accessible temperature (2 K). After temperature stabilization, a magnetic field of 50 Oe was applied and the magnetization recorded as the temperature was raised (ZFC curve) up to 200 K. Then the measurement continued while the temperature was decreased back to 2 K (FC curve), keeping the same applied magnetic field. For all samples the ZFC curves come below the FC ones, as indicated in figure 4 for the undoped ($x = 0$) sample. Again the results for lightly and heavily doped samples are presented in different panels (figures 4(a) and (b), respectively). For a substitution of 10% of Ru atoms by Nb ($x = 0.1$), we observe that the overall shape of the magnetization curve is similar to the result obtained for the undoped sample, although some important differences between these two curves can be pointed out. For instance, the peak in the ZFC curve associated with the cluster glass (CG) transition is strongly shifted to lower temperatures, as already observed in the AC susceptibility measurements. Also, at low temperatures and $x \geq 0.1$, the stronger diamagnetic signal from the superconducting phase turns the ZFC curve negative and causes a small reduction of the magnetization in the FC curve. More dramatic changes can be observed for the samples with $x \geq 0.2$. For those samples, the CG peak in the ZFC curve is not present, indicating that the glassy transition is completely suppressed. There is a dramatic reduction in the magnetic moment associated with the Ru sublattice making the superconducting signal more prominent. Curiously, the superconducting diamagnetic signal becomes weaker with the increase of niobium content, for $x \geq 0.2$, indicating a smaller superconducting fraction, in agreement with the AC susceptibility results. The reduction in the superconducting fraction also follows the trend observed for T_c extracted from resistivity and AC susceptibility measurements, where a peak was observed for $x = 0.2$ (see figure 2(b)). For $x \leq 0.1$ the superposition of the magnetic and superconducting responses makes it difficult to estimate the change in the superconducting fraction from DC magnetization.

The reduction in the superconducting fraction and in T_c with the increase of niobium content, for $x \geq 0.2$, can be explained by the change in the carrier density transfer to the CuO_2 planes with doping, which affects the superconducting properties. But the most striking feature of the magnetization curves presented in figure 4, and also in the AC susceptibility results of figure 3, is that there is a critical doping level, around $x = 0.2$, which separates the samples into two very distinct magnetic behaviours. For $x < 0.2$ the samples present a spin glass-like transition and high magnetic moments, while for $x \geq 0.2$ this transition is completely suppressed and the total magnetic moment becomes smaller by about one order of magnitude. This may explain the maximum in T_c for $x = 0.2$, observed both in the resistivity and magnetic measurements. Considering only the changes in the carrier density we would expect T_c (and the superconducting fraction) to be maximum for $x = 0.0$, and to decrease with the increase in niobium concentration up to $x = 0.5$. However, the much higher magnetic moments occurring for the samples with $x \leq 1$ act as Cooper pair-breakers, thus reducing T_c as well as the superconducting fraction. Our results confirm the conclusions presented in [22],

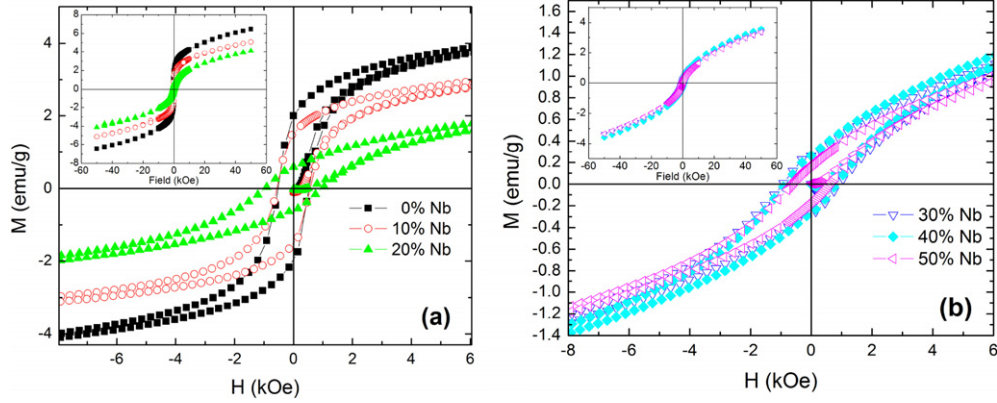


Figure 5. Magnetic hysteresis loops for lightly (a) and heavily (b) Nb-doped Ru-1222 samples, measured at $T = 2$ K. The main panels show the central part of the loops, while the insets present the complete curves. Notice that the magnetic loops are insensitive to the Nb content for heavily doped samples.

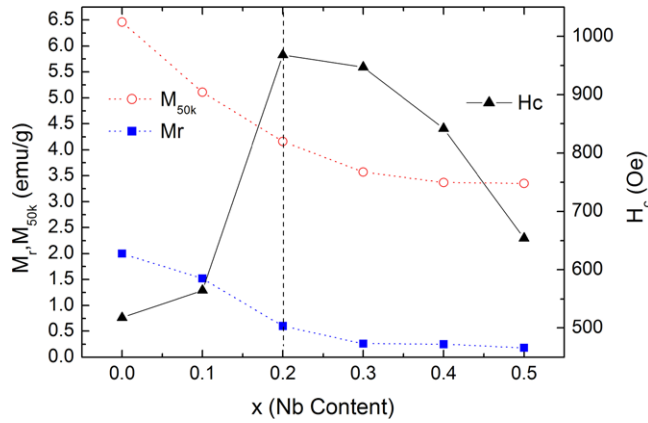


Figure 6. Dependence of the coercive field (H_c , right axis), remanent magnetization and magnetization at 50 kOe (M_r and M_{50k} , respectively, left axis) with niobium doping.

where Mo-doped Ru-1222 samples were studied. In the case of Mo^{6+} doping, the changes in T_c were significantly more prominent than in the present Nb doping case, due to the larger change in the carrier density. The presence of a pair-breaking effect was also identified for Mo doping and modelled using the Abrikosov–Gorkov theory for magnetic impurities [22].

The substitution of ruthenium by niobium also induces significant changes in the low temperature ($T = 2$ K) magnetic hysteresis loops, as shown in figure 5. The loops for samples $x = 0$ and $x = 0.1$ are similar, differing basically by the magnitude of the magnetization (see figure 5(a)). In fact, if these two curves are normalized by the corresponding magnetization at 50 kOe, they collapse in a single curve (not shown). Increasing the niobium content to $x = 0.2$ causes a significant change in the shape of the hysteresis loop, particularly by increasing the coercive field. Further increases in the niobium concentration barely affect the hysteresis loops (see figure 5(b)). The remanent magnetization (M_r), magnetization at $H = 50$ kOe (M_{50k}) and coercive field (H_c), extracted from the magnetic hysteresis loops for all samples, are plotted in figure 6. The magnetization does not really saturate up to the maximum available field of

50 kOe, so we plotted M_{50k} instead of the saturation magnetization. As the content of niobium in the samples increases, M_r and M_{50k} decrease, reaching an almost constant value for samples with $x \geq 0.3$, with a prominent change in M_r when the Nb content increases from $x = 0.1$ to 0.2. However, the most striking features presented in figure 6 are the jump in H_c when the Nb content increases from $x = 0.1$ to 0.2, and the insensibility of the hysteresis loops for $x \geq 0.3$. It is important to notice that the samples for $x \geq 0.2$ do not present the cluster glass transition. Therefore, one could analyse the presented magnetization loops to be a result of two separate contributions. One of them (dominant for $x > 0.2$) could be associated with the canted antiferromagnetic phase, which produces broader magnetic loops with smaller magnetizations at 50 kOe. Those loops are mostly insensitive to Nb doping, pointing to small changes in the antiferromagnetic phase. The second contribution comes from the cluster glass phase. This contribution (dominant for $x \leq 0.2$) increases the magnetization at high magnetic fields and is very sensitive to the level of Nb doping. Therefore, the observed loops provide evidence for the existence of different regions in the sample, which present essentially independent magnetic behaviours. Such interpretation has recently been proposed to explain the complex magnetic response of Ru-1222 [6–10]. According to [10], the presence of oxygen vacancies may favour the ruthenium ions around it to assume valence 4+, instead of the usual 5+. This would lead to the formation of Ru⁴⁺-rich clusters, which would present different magnetic interaction compared to the rest of the matrix. Our results fit nicely into this picture, considering that the matrix orders antiferromagnetically and that the Ru⁴⁺-rich clusters freeze into a cluster glass at the temperature defined by the peak in the real part of the AC susceptibility. Therefore, the strong suppression of the cluster glass transition with Nb substitution may come from an increase in the overall oxygen content in heavily Nb-substituted samples. This is also consistent with our previous results that showed an increase in the blocking temperature of the glassy transition, when the oxygen content of the sample was reduced [6]. The Nb substitution could provide some dilution effect in the Ru sublattice as well, since some Ru ions had been removed and the average separation between them had increased. However, the fact that the hysteresis loops do not change appreciably for $x > 0.2$ indicates that the increase in Nb content does not meaningfully affect the AFM order for heavily substituted samples. One last alternative to be analysed is the possible influence of magnetic impurities on the obtained results. Although the XRD data indicate the presence of small amounts of RuSr₂GdCu₂O₈ and RuSr₂GdO₆ in all samples, it is unlikely that such impurities could produce the robust magnetic loops we observed. Also, the number of impurities changes from sample to sample and we should be able to observe some correlation between the number of impurities and the magnetic response of the samples, which is not the case. Therefore, we conclude that the number of impurities in our samples is not sufficient to produce any measurable influence in our results.

4. Final remarks

In this work we have explored the influence of ruthenium substitution by niobium on the electrical and magnetic properties of polycrystalline samples of Ru_{1-x}Nb_xSr₂Gd_{1.5}Ce_{0.5}Cu₂O_{10-δ} (Ru-1222:Nb). It was observed that niobium substitution strongly reduces the cluster glass transition temperature, which becomes completely suppressed for samples with $x \geq 0.2$. The antiferromagnetic transition observed at $T \approx 160$ K was found to be only marginally affected by this substitution. By increasing the Nb content, we also observed an increase (up to $x = 0.2$) followed by a decrease in the superconducting transition temperature (T_c), as shown in figure 2(b). We explain this behaviour through a decrease in the carrier density, caused by the increase of Nb doping, combined with a pair-breaking effect of the strong magnetic moment present in the samples with $x = 0.0$ and 0.1. Therefore, we verified that the magnetic moment

does interfere in the superconducting properties of Ru-1222:Nb samples, in contrast to previous studies that indicated both phenomena to be decoupled [26, 27]. However, the suppression of T_c attributed to the magnetic order is relatively small and may have easily been overlooked in previous studies. In contrast, our results by no means conflict with the results reported in [18], where the Zn substitution for Cu in Ru-1222 was studied. In [18] the superconductivity was found to be suppressed and it was also verified that the magnetic order was not affected. Here we propose that changes in the magnetic order could affect the superconducting properties simply by a pair-breaking effect, without evoking any deeper correlation between magnetic order and superconductivity.

It is also interesting to compare our results with previous works on doped Ru-1212 [29]. The dependence of T_c with doping in Ru-1212 compounds may be explained solely by changes in the carrier density, since the magnetic moment in these samples is too weak to provide a measurable effect on T_c . It is important to notice that it was only in Ru-1222 that the presence of a cluster glass phase was observed; this is not present in Ru-1212. Therefore, this can explain why it is possible to observe the pair-breaking effects reported here for the Ru-1222 system. Also, the magnetic hysteresis loops provide additional evidence that the magnetic behaviour of the Ru-1222:Nb samples may be interpreted as a combination of two separate contributions: one coming from the canted antiferromagnetic matrix and the other from the Ru⁴⁺-rich clusters around oxygen vacancies which would lead to the glassy transition at lower temperatures. Both contributions could be clearly identified in this work because the niobium substitution affected each of them differently.

In conclusion, we have observed the partial suppression of superconductivity in lightly Nb-doped Ru_{1-x}Nb_xSr₂Gd_{1.5}Ce_{0.5}Cu₂O_{10-δ} samples ($x \leq 0.1$), due to the presence of strong magnetic moments. As the niobium concentration increases the CG phase is strongly suppressed, disappearing completely for $x \geq 0.2$. The non-monotonic dependence of T_c with x may be explained by a combination of the pair-breaking effect of the magnetic moment, for $x \leq 0.1$, and the reduction of charge carrier concentration in the CuO₂ planes, for $0 \leq x \leq 0.5$. We could also observe two distinct contributions to the total magnetic moment in these samples, one coming from an antiferromagnetic phase and another from a cluster glass phase.

Acknowledgments

This work was supported by the Brazilian agencies FAPESP and CNPq. Authors from the NPL appreciate the interest and advice of Professor Vikram Kumar (Director) in the present work.

References

- [1] Felner I, Asaf U, Levi Y and Millo O 1997 *Phys. Rev. B* **55** R3374
- [2] Tokunaga Y, Kotegawa H, Ishida K, Kitaoka Y, Takagiwa H and Akimitsu J 2001 *Phys. Rev. Lett.* **86** 5767
- [3] Awana V P S, Karppinen M and Yamauchi H 2003 *Studies of High T_c Superconductors* ed A V Narlikar (New York: Nova Science) p 77
- [4] Cardoso C A, Araujo-Moreira F M, Awana V P S, Takayama-Muromachi E, de Lima O F, Yamauchi H and Karppinen H 2003 *Phys. Rev. B* **67** 020407(R)
- [5] Cardoso C A, Araujo-Moreira F M, Awana V P S, Kishan H, Takayama-Muromachi E and de Lima O F 2004 *Physica C* **405** 212
- [6] Cardoso C A, Lanfredi A J C, Chiquito A J, Araujo-Moreira F M, Awana V P S, Kishan H, de Almeida R L and de Lima O F 2005 *Phys. Rev. B* **71** 134509
- [7] Felner I, Galstyan E, Herber R H and Nowik I 2004 *Phys. Rev. B* **70** 094504
- [8] Shengelaya A, Khasanov R, Eschenko D G, Felner I, Asaf U, Savić I M, Keller H and Müller K A 2004 *Phys. Rev. B* **69** 024517
- [9] Xue Y Y, Cao D H, Lorenz B and Chu C W 2001 *Phys. Rev. B* **65** 020511(R)

- [10] Felner I, Galstyan E and Nowik I 2005 *Phys. Rev. B* **71** 064510
- [11] Garcia S, Ghivelder L, Soriano S and Felner I 2006 *Eur. Phys. J. B* **53** 307
- [12] Lopez A, Azevedo I S, Gonzalez J L, Baggio-Saitovich E and Micklitz H 2006 *Physica C* **442** 33
- [13] Matvejeff M, Awana V P S, Jang L-Y, Liu R S, Yamauchi H and Karppinen M 2003 *Physica C* **392** 87
- [14] Živković I, Hirai Y, Frazer B H, Prester M, Drobac D, Ariosa D, Berger H, Pavuna D, Margaritondo G, Felner I and Onellion M 2002 *Phys. Rev. B* **65** 144420
- [15] Fainstein A, Winkler E, Butera A and Tallon J 1999 *Phys. Rev. B* **60** R12 597
- [16] Williams G V M and Krämer S 2000 *Phys. Rev. B* **62** 4132
- [17] Butera A, Fainstein A, Winkler E and Tallon J 2001 *Phys. Rev. B* **63** 054442
- [18] Felner I and Galstyan E 2003 *Int. J. Mod. Phys. B* **17** 3617
- [19] Shi L, Li G, Feng S J and Li X-G 2003 *Phys. Status Solidi a* **1** 137
- [20] Shi L, Li G, Pu Y, Zhang X D, Feng S J and Li X-G 2003 *Mater. Lett.* **57** 3919
- [21] Lee H K, Park H M and Williams G V M 2005 *Int. J. Mod. Phys. B* **19** 353
- [22] Awana V P S, Lal R, Kishan H, Narlikar A V, Peurla M and Laiho R 2006 *Phys. Rev. B* **73** 014517
- [23] Awana V P S, Kishan H, Eshkenazi O, Felner I, Rawat R, Ganesan V and Narlikar A V 2007 *J. Phys.: Condens. Matter* **19** 026203
- [24] Kalavathi S, Janaki J, Sairam T N, Maui A, Rawat R and Sastry V S 2006 *Solid State Commun.* **139** 334
- [25] Goh S K, Williams G V M and Lee H K 2006 *Curr. Appl. Phys.* **6** 515
- [26] Lee H K and Kim Y C 2003 *Int. J. Mod. Phys. B* **17** 3682
- [27] Lee H K and Williams G V M 2004 *Physica C* **415** 172
- [28] Rijssenbeek J T, Mansourian-Hadavi N, Malo S, Ko D, Washburn C, Maignan A, Pelloquin D, Mason T O and Poepelmeier K R 2000 *Physica C* **341** 481
- [29] Williams G V M, Lee H K and Krämer S 2003 *Phys. Rev. B* **67** 104514
- [30] McLaughlin A C, Janowitz V, McAllister J A and Attfield J P 2000 *Chem. Commun.* **14** 1331
- [31] Liu R S, Jang L-Y, Hung H-H and Tallon J L 2001 *Phys. Rev. B* **63** 212505
- [32] Williams G V M, Jang L-Y and Liu R S 2002 *Phys. Rev. B* **65** 64508
- [33] Hu Z, von Lips H, Golden M S, Fink J, Kaindl J, de Groot F M F, Ebbinghaus S and Reller A 2000 *Phys. Rev. B* **61** 5262
- [34] Goldfarb R B, Lelental M and Thompson C A 1991 *Susceptibility of Superconductors and Others Spin Systems* ed R A Hein, T L Francavilla and D H Lieberger (New York: Plenum) p 49